Office of the Chief of Naval Research
Contract N00014-87-K-0326
Technical Report No. UWA/DME/RT-90/3

A SEM PROCEDURE FOR QUANTIFYING TRANSGRANULAR FRACTURE IN BRITTLE MATERIAL

W.-J. Yang, C.-T. Yu and A. S. Kobayashi

July 1990

The research reported in this technical report was made possible through support extended to the Department of Mechanical Engineering, University of Washington, by the Office of Naval Research under Contract N00014-K-0326. Reproduction in whole or in part is permitted for any purpose of the United States Government.

DISCLAIMER NOTICE

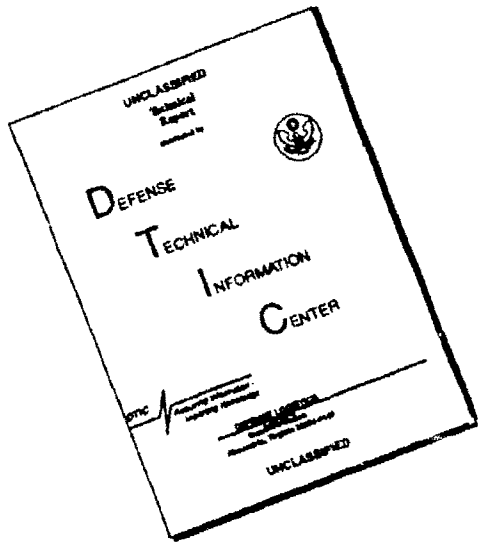

THIS DOCUMENT IS BEST QUALITY AVAILABLE. THE COPY FURNISHED TO DTIC CONTAINED A SIGNIFICANT NUMBER OF PAGES WHICH DO NOT REPRODUCE LEGIBLY.

07-11-90

A SEM PROCEDURE FOR QUANTIFYING TRANSGRANULAR FRACTURE IN BRITTLE MATERIAL

Wein-Joe Yang, Chang-Te Yu and Albert S. Kobayashi
University of Washington
Department of Mechanical Engineering
Seattle, WA 98195

ABSTRACT

A SEM procedure for quantifying the percentage area of transgranular fracture was developed for studying the fracture morphologies of stable and rapid crack growths in ceramics and ceramic matrix composites. The procedure utilizes SEM line scanning profiles which are scanned and then interpreted as percentage area of transgranular fracture and surface roughness through a special software. This procedure was used to quantify the percentage area of transgranular fracture and surface roughness which were correlated with the visual observations and profilometer measurements respectively, of Al_2O_3 and SiC_w/Al_2O_3 fracture specimens.

INTRODUCTION

Dynamic fracture of quasi-brittle metals and polymers are characterized by crack velocity versus stress intensity factor (SIF) relations which represent a gamma curve with distinct crack arrest SIF's, [1-4]. Conventional dynamic fracture tests show unequivocally that unlike metals/polymers, such dynamic crack arrest SIF does not exist in monolithic and some ceramic matrix composites[5-12]. These results were generated by blunt machined notches with larger stored energy prior to rapid crack propagation. Once the excess driving force had been dissipated during rapid crack propagation under static loading and the crack had entered a region of dynamic SIF, which is lower than K_{IC}, crack arrest was to be expected but such was not the case. Crack arrest, however, has been observed in chevron-notched, SiC_w/Al_2O_3 ceramic composites, three point bend specimens, when loaded under an extremely small displacement rate of 0.01 mm/min. [13]. The run-arrest events in these tests were characterized by small crack jumps of about 0.8 mm, which initiated at the sharp crack tip in the chevron notched specimens.

Recently, this lack of crack arrest was attributed to the small difference in the fracture morphology associated with extremely slow and rapid crack extensions. This postulate was tested by extensive fractography analysis of the statically and impact loaded Al_2O_3 specimens [14]. Typical SEM pictures of the fracture surfaces from the

crack initiation and the terminal phases of statically loaded Al_2O_3 specimen showed that while intergranular fracture was the dominant failure mode in both specimens, differing amount of transgranular fracture was observed on the fracture surface. The percentage areas of transgranular fracture decreased from an average of 16% during the initiation phase to an average of 10% at slower crack propagation in the impacted specimen. For a statically loaded specimen, the percentage areas of transgranular fracture during the initiation and crack propagation phases were 5 and 2%, respectively. The higher percentage areas of transgranular fracture during the initiation phase was attributed to the higher crack velocity and the higher dynamic SIF due to the excessive driving force generated by the blunt crack tip. This fractography analysis also showed that rapid crack propagation is always accompanied by transgranular fracture regardless of the magnitudes of the dynamic SIF and the crack velocity. Unfortunately, no comparison could be made with the fracture morphology associated with stable crack growth since these test results consisted of only rapid crack propagation events even in the statically loaded specimen.

The above finding regarding transgranular fracture is consistent with those observed by others [15,16] and more recently by Nose et al [17] who reported not only transgranular failure of the Al_2O_3 matrix but also SiC whisker failure under rapid crack propagation, i.e. pop-in, in the SiC_w/Al_2O_3-matrix composite. In contrast, the fracture morphology for stable crack growth in [17] showed the dominance of intergranular failure accompanied by SiC whisker pull-outs. The SIF for the former, i.e. pop-in fracture or rapid crack propagation, remained a constant 6 $MPa\sqrt{m}$ while the SIF continued to increase to about 9 $MPa\sqrt{m}$ with increased stable crack extension. In a previous paper [18], Nose et al also reported similar findings of a lower SIF of about 4 $MPa\sqrt{m}$ associated with pop-in fracture and a higher SIF varying from 4 to 5.5 $MPa\sqrt{m}$ associated with subcritical crack growth in Al_2O_3.

Since the percentage area of transgranular fracture is related to the instantaneous dynamic fracture toughness of ceramics and ceramic composites as the above results [14-18] suggest, this quantity must be measured. This paper reports on a SEM procedure for estimating the percentage area of transgranular fracture on the fracture surface of ceramics and ceramic composite.

METHODOLOGY

The procedure is based on the assumption that the plane of transgranular fracture will be in the crack plane as shown in Figure 1a. Intergranular fracture, on the other hand is characterized with a tilt in the crack surface as shown by Figure 1(b). Figure 1(a) also shows that this assumption cannot discriminate the intergranular fracture surface when it coincides with the dominant crack plane.

The method of approach is to relate the topology of the fracture surface, i.e. the non- or slightly tilted fracture surfaces whose lengths exceed the average grain size of the ceramic matrix material. Stereophotogrammetry and profilometry are known procedures [19] which can be used for this purpose. In this paper, we present a third procedure which utilizes the line scanning profile of a scanning electron microscope (SEM).

SEM Scanning Line Profile

The topography of the fracture surface in Figure 2(a) is first recorded by line scanning of the intensity of the secondary electrons (SE) emitted by normal incidence of the electron beam in a SEM. The relative variation in the SE intensity or the contrast is recorded as the variation in the line scanning profile (LSP). This contrast increases with the tilt of the fracture surface to the normal incident electron beam where a larger number of SE's are emitted with a steeper tilt as shown schematically in Figure 2(b). The ratio of SE's from the tilted to normal surfaces follows the secant law [20] with negligible change in contrast for tilt. The solid line indicates the SE signal collected by the SEM detector. The dotted lines represent the local intensity of collection. The simulated profile of Figure 2(c) is established by summing up the intensity of the signals. At the intersections of segments, the profile is distorted by spikes which can be filtered later during the spectral analysis.

Transgranular fracture area can be defined from the LSP record as a constant slope segment with a length longer than the average grain size where the contract increases with an increasing tilt angle. For a ceramic matrix composite with whiskers, the resultant spikes among the constant contrast in the LSP is also distorted by the whiskers but can be filtered out in the subsequent analysis.

A multitude of line scanning profiles (LSP) are therefore taken by using a JEOL SEM T-330 instrument. The LSP's are then scanned by a AST-TURBOSCAN/MAC-SCAN and digitized for subsequent data analysis.

Spectral Analysis

Spectral analysis of the LSP is necessary to eliminate the spikes caused by the grain boundaries and the distortion caused by whisker/fiber breakages and pullouts. Fast Fourier transform (FFT) was used to compute the coefficients of a discrete Fourier series and the frequency distribution of the random process. This spectral analysis also provides the root mean square of the surface roughness which can be deduced from the LSP.

Procedure

Figure 3 shows the flow chart for determining the percentage area of transgranular failure and the roughness. The first step is to obtain a series of LSP's under the same contrast setting at the prescribed region. As mentioned previously, the LSP are scanned by an AST-TURBOSCAN and digitized by the MAC-SCAN program which locates the Y-coordinate in contrast setting along the X-coordinate of the scanning distance. The program, LSP-SLOP then transforms the X-Y coordinate data file and calculates the percentage area of transgranular failure. An input parameter to the LSP-SLOP program is the length in the X-coordinate which must be excluded in order to eliminate material inhomogeneities, such as fiber breakage, and unusual contrast. Another input length parameter is the average grain size of the ceramic matrix which is needed to detect segments of transgranular fracture. LSP-SLOP thus scans the lengths of all horizontal and tilted line segments, which exceeds this average grain size, and computes the percentage area of transgranular fracture. Details of the procedure and the softwares involved are provided in [21].

QUANTITATIVE FRACTOGRAPHY OF Al_2O_3 And SiC_w/Al_2O_3 COMPOSITE

The specimen used to demonstrate the utility of this procedure is a wedge-loaded double cantilever beam (WL-DCB) specimen with a long chevron notch as shown schematically in Figure 4(a). The inherent rigidity of the WL-DCB specimen plus the long

chevron notch makes it ideal for studying stable crack growth followed by crack jump with run-arrest under a slow displacement controlled loading. The latter is identified by a distinct shade in the texture of the fracture surface as shown by the SEM photo in Figure 4(b).

LSP Versus SEM Photos

Figure 5 shows a SEM photograph of a Al_2O_3 with a superimposed LSP along the center line. A visual comparison of the SEM record and the LSP shows that the variation in intensity of the LSP closely follows the variation of the surface topology as deciphered from the photograph. Figure 6 shows a similar record for the SiC_w/Al_2O_3 composite. The whiskers and grain boundaries in Figure 6 appear brighter than the matrix grain surfaces due to the higher conductivity of SiC and the static charges along the grain boundaries. The LSP in Figure 5 contains less spikes than those of Figure 6 due to the lack of whiskers in the former. If the peaks in the LSP's are removed, then the LSP in Figure 5 will be even closer to the real surface profile. These peaks are removed by the spectral analysis as mentioned previously. In all the SEM records studied, large transgranular fracture area exhibited a constant slope, which is nearly equal to zero in Figures 5 and 6, and the surrounding grain boundaries had little effect on the intensity of SE.

Processing LSP

Since the brightness control on the SEM has no effect on the contrast, it has no influence on the LSP. Figure 7 illustrates this point where each LSP was taken under 1000X magnification with identical setting of the contrast level. The material and type of fracture, i.e. stable versus rapid crack growth are denoted in the captions. By changing the brightness level, the LSP will move up or down on the SEM screen without altering the contrast level and thus many LSP's can be shown in one record as shown in Figure 7. On the other hand, Figure 8 shows the scanned and digitized individual LSP's which are processed by the LSP-SLOP and the FFT programs. A comparison of Figures 7 and 8 show that the LSP's of a 25% SiC_w/Al_2O_3 composite have more spikes but also exhibits a smoother profile. Apparently, the LSP profile of Al_2O_3 is much rougher than that of a 25% SiC_w/Al_2O_3 composite.

Percentage Areas of Transgranular Fracture

Percentage area of transgranular fracture is calculated by the program LSP-SLOP. Each processed LSP record provides a percentage area of transgranular fracture and the root mean square of the roughness. Slight differences in the geometry and the loading history are the probable cause for the differences, as shown in Table 1, between the two specimens. The SEM photographs of the two 25% SiC_w/Al_2O_3 composite specimens shows that the fractured surface of the first specimen is more distinct and has smoother rapid crack growth zones than those of the second one. The slightly higher percentage area of transgranular fracture in the first specimen is due to this slight difference in fracture morphology. The percentage areas of transgranular fracture were obtained visually by examining ten SEM records at 5000X magnification or two SEM records at 1000X magnification and identifying the transgranular fracture area. This process is easier for alumina than for SiC_w/Al_2O_3 composite. The percentage areas of transgranular fracture in Al_2O_3 in Table 1 is very close to that obtained previously [14].

Roughness

Spectrum analysis was carried out by the FFT program. The LSP spectral density plots of stable and rapid crack growth regions in the Al_2O_3 and SiC_w/Al_2O_3 composite are shown in Figures 9 and 10. The spectral frequencies varied, but concentrated in the lower which range varied from approximately 0.5 (l/μm) to a very low frequency. This frequency corresponds to one grain size of 2μm to 10μm or higher.

Distortion of the LSP due to the edge effect and fiber perturbations lies in the frequency range of 1.0 (1/μm) and are higher since the whisker diameter is about 0.5μm. The length of the distorted intervals range from 0.5μm to 1μm if the orientation of the fibers is considered. The filtered frequency ranges from 1.0 (l/μm) and above. In contrast, Al_2O_3 has a lower intensity of distortion when the edge distortion is around 0.4μm or lower and its effect on the whole spectral density area can thus be neglected.

As described previously, the area under the LSP spectral density distribution is proportional to the root-mean-square of the profile. To minimize signal distortion, a band-pass filter was inserted to purge the aliasing frequencies prior to calculating this

area. Once the areas are obtained, a correction factor is multiplied to find the root-mean-square roughness. This 'correction' factor can be obtained by comparing the LSP's of a polished surface with the measured roughness data obtained by a Federal 400 profilometer. For Al_2O_3 material, the roughness ranges from 0.30-0.32μm in the stable crack region and 0.23 - 0.25μm in the rapid crack growth region. For the SiC_w/Al_2O_3 composite, it is from 0.24 - 0.25μm in the stable crack region and 0.20 - 0.21μm in the rapid crack growth region.

This procedure based on spectral density provides a technique of noncontact profilometry. It has two main advantages. First, specimens will not be scratched by the diamond probe used in conventional roughness measurement. Second, this procedure is not limited by the height of crack deflection of probe which has its range of stroke and height deviations.

CONCLUSIONS

1. A SEM procedure for quantifying the percentage area of transgranular fracture and roughness was established.

2. The percentage area of transgranular fracture in Al_2O_3 and SiC_w/Al_2O_3 composite in the rapid crack growth region were lareger than those in the stable crack growth region.

3. The fractured surfaces of SiC_w/Al_2O_3 composite are smoother than the corresponding surfaces in Al_2O_3.

4. LSP spectral analysis showed that crack deflection was more prevalent in the stable crack growth region.

ACKNOWLEDGEMENT

This research was supported by the Office of Naval Research Contract No. 0004-87-K0326. The authors express gratitude to Drs. Yapa Rajapakse and Steve Fishman for their patience and encouragement during the course of this investigation.

REFERENCES

1. Kobayashi, T. and Dally, J.W., "Dynamic Photoelastic Determination of the $\dot{a}$-K Relation for 4340 Alloy Steel," Crack Arrest Methodology and Applications, G.T. Hahnard, M.F. Kanninen (eds), ASTM STP 711, 1980, pp. 189-210.

2. Kalthoff, J.F., Beinert, J., Winkler, S. and Klemm, W., "Experimental Analysis of Dynamic Effects in Different Crack Arrest Test Specimens," G.T. Hahn and M.F. Kannin, (eds), ASTM STP 711, 1980, 109-127.

3. Dally, J.W., "Dynamic Photoelastic Studies of Fracture," Experimental Mechanics, Vol. 19, 1979, pp. 349-361.

4. Kobayashi, A.S., Ramulu, M., Dadkhah, M.S., Yang, K.H., and Kang, B.S.-J., "Dynamic Fracture Toughness," Intl. J. of Fracture, 30, 1986, pp. 275-285.

5. Kobayashi, A.S., Emery, A.F. and Liaw, B.M., "Dynamic Toughness of Glass," Fracture Mechanics of Ceramics, Vol. 6 eds R.C. Bradt, A.G. Evans, D.P.H. Hasselman and F.F. Lange, Plenum Press, 1983, pp 47-62.

6. Kobayashi, A.S., Emery, A.F., and Liaw, B.M., "Dynamic Fracture Toughness of Reaction Bonded Silicon Nitrode," J. American Ceramic Soc., Vol. 66, No. 2, 1983, pp. 151-155.

7. Liaw, B.M., Kobayashi, A.S., and Emery, A.F., "Effect of Loading Rates on Dynamic Fracture of Reaction Bonded Silicon Nitride," Fracture Mechanics: Seventh Volume ASTM STP 905, 1986, pp.95-107.

8. Kobayashi, A.S., Yang, K.-H. and Emery, A.F., "Dynamic Fracture Testing of Alumina," Impact Loading and Dynamic Behavior of Materials, C.Y. Chiem, H.-D. Kunze and L.W. Meyer (eds.) DGB Informationsgesellschaft mgH, 1988, pp. 113-119.

9. Yang, K.-H., Kobayashi, A.S. and Emery, A.F., "Dynamic Fracture Characterization of Ceramic Matrix Composites," Journal de Physique, Colloque C3, supplément au No. 9, 1988, C3-223-230.

10. Yang, K.-Y., Kobayashi, A.S. and Emery, A.F., "Effects of Loading Rates and Temperature on Dynamic Fracture of Ceramics and Ceramic Matrix Composites," American Ceramic Society Ceramic Materials and Components for Engines, V.J. Tennery and M.K. Ferber (eds.), 1989, pp. 766-775.

11. Kobayashi, A.S. and Yang, K.-H., "A Hybrid Technique for High-Temperature Dynamic Fracture Analysis," Proc. of International Conference on Advanced Measurement Techniques, London, August 25-27, 1987.

12. Yang, K.H. and Kobayashi, A.S., "An Experimental-Numerical Procedure for High Temperature Dynamic Fracture Analysis," Computational Mechanics '88, ed. S.N. Atluri and G. Yagawa, Springer-Velag, 1988, pp 48.v.1-8.

13. Jenkins, M.G., Kobayashi, A.S., White, K.W. and Bradt, R.C., "Crack Initiation and Arrest in SiC Whisker/Al_2O_3 Matrix Ceramic/Ceramic Composites," Journal of Americal Ceramic Society, Vol. 70, No. 6, June 1987, pp. 393-395.

14. Yang, K.H. and Kobayashi, A.S., "Dynamic Fracture Responses of Alumina and Two Ceramic Composites," to be published in Journal of American Ceramic Society.

15. Mecholsky, J.J. and Freiman, S.W., "Fractographic Analysis of Delayed Failure in Ceramics," Fractography and Materials Science, eds. I.N. Gilbertson and R.D. Zipp, ASTM STP 733, 1981, pp 246-258.

16. Healey, J.T. and Mecholsky, J.J., "Scanning Electron Microscopy Techniques and Their Application to Failure Analysis of Brittle Materials," Fractography of Ceramic and Metal Failures, ed. J.J. Mecholsky and S. R. Powell, ASTM STP 827, 1984, pp 157-181.

17. Nose, T., Ueki, M., Fujii, T. and Kubo, H., "Toughening Behavior in SiC Whisker Reinforced Al_2O_3 Ceramics," a paper presented at 1st International Ceramic Science & Technology Congress, Oct 31-Nov. 3, 1989, Anaheim, CA.

18. Nose, Tetsuro and Fujii, Toshimitsu, "Evaluation of Fracture Toughness for Ceramic Materials by a Single-Edge-Precracked-Beam Method," Journal of the American Ceramic Society, Vol. 71, No. 5, pp 328-333, June 1988.

19. Underwood, E.E., "Recent Advances in Quantitative Fractography," Fracture Mechanics: Microstructure and Micromechanisms, eds. S.V. Nair, J.K. Tien, R.C. Bates and O. Buck, ASM International, 1989, pp 87-109.

20. Newbury, D.E. and Yokowitz, H., "Studies of the Distribution of Signals in SEM/EPMA by Monte Carlo Calculations in Electron Probe Microanalysis and Scanning Electron Microscopy, National Bureau of Standards, 1976, pp. 15- 43.

21. Yang, Wein-Joe, "Quantitative Fractography Study of Brittle Materials," a MSME thesis submitted to the University of Washington, 1990.

ASK/cm/7/11/90

Table 1. Percentage Areas of Transgranular Fracture

Procedure	Crack Growth	
	Stable	Rapid
This Procedure		
Al_2O_3		
Specimen 1 (Region 1)	10%	17%
Specimen 2 (Region 2)	12%	15%
Visual Processing		
Specimen #1	13%	19%
This Procedure		
25% SiC_w/Al_2O_3		
Specimen #2	42%	73%
Specimen #5	43%	58%
Visual Processing		
25% SiC_w/Al_2O_3		
Specimen #2	37%	73%

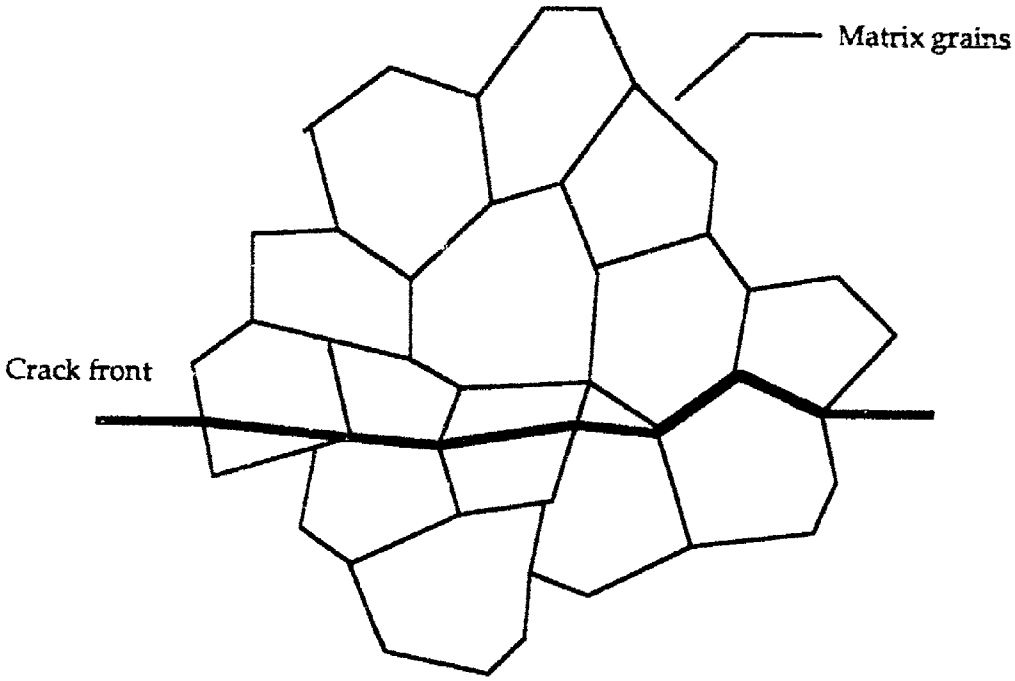

(a) Trans-and Intergranular Fracture

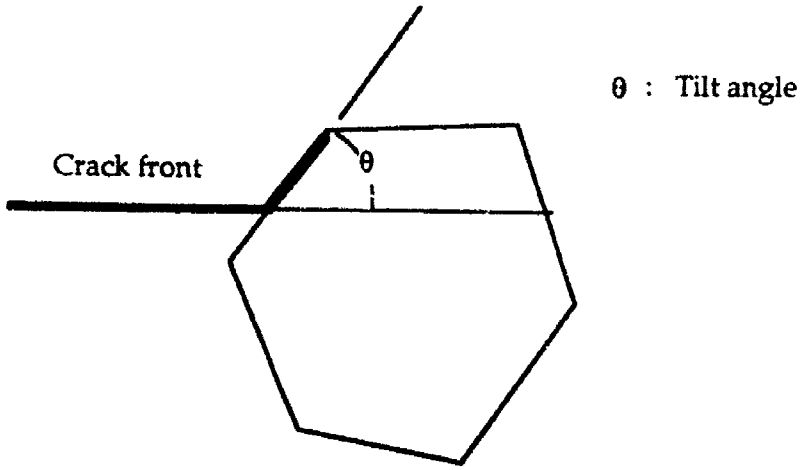

(b) Intergranular Fracture

Figure 1. Crack Propagation in Matrix Grain

(a) Idealized 2-D Fracture Surface

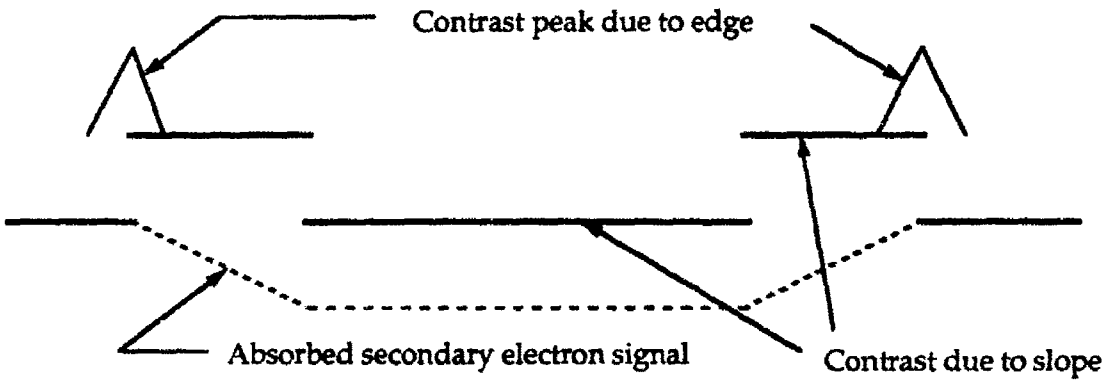

(b) Secondary Electron Emission

(c) Simulated Fracture Surface

Figure 2. Fracture Surface Simulation by Secondary Electron Emission Profile

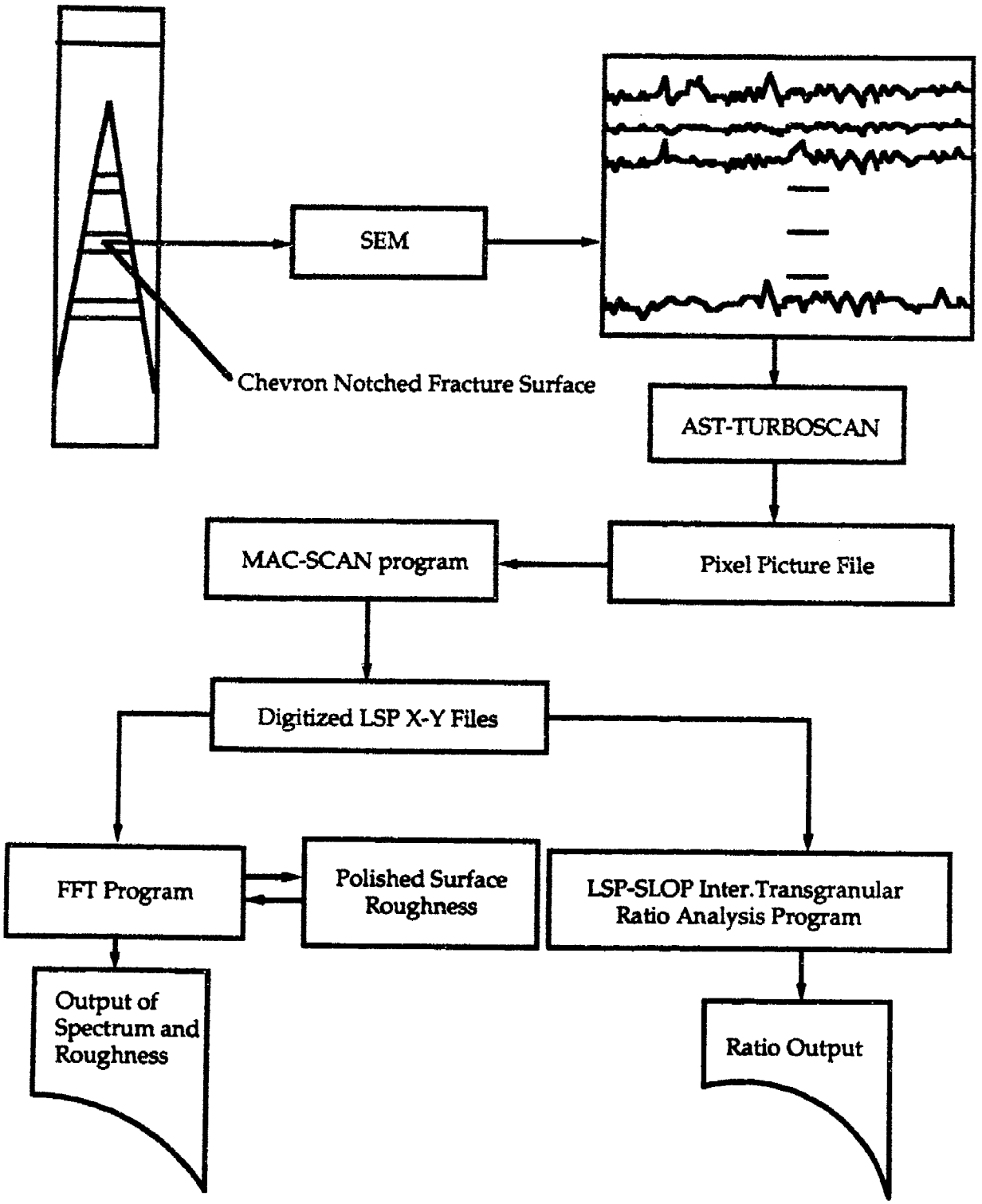

Figure 3. Flow Chart of Procedure

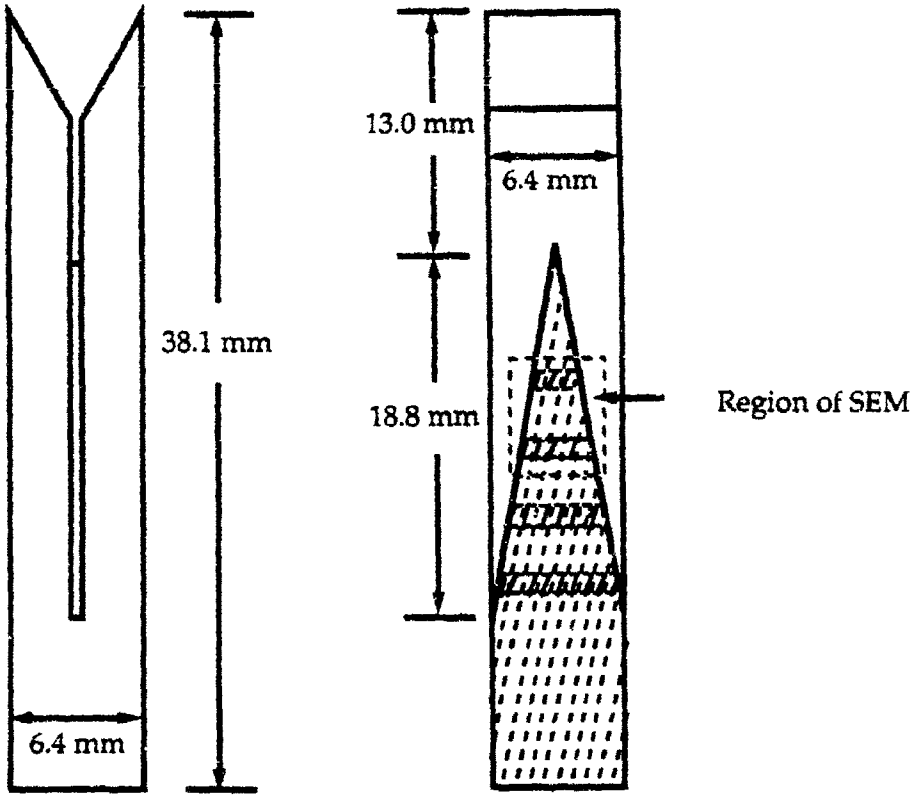

(a) Chevron Notched Wedge-Loaded Double Cantilever Beam Specimen

(b) SEM of the Above

Figure 4. Fracture Surfaces Associated With Slow and Fast Crack Propagation.

(a) Stable Crack Growth

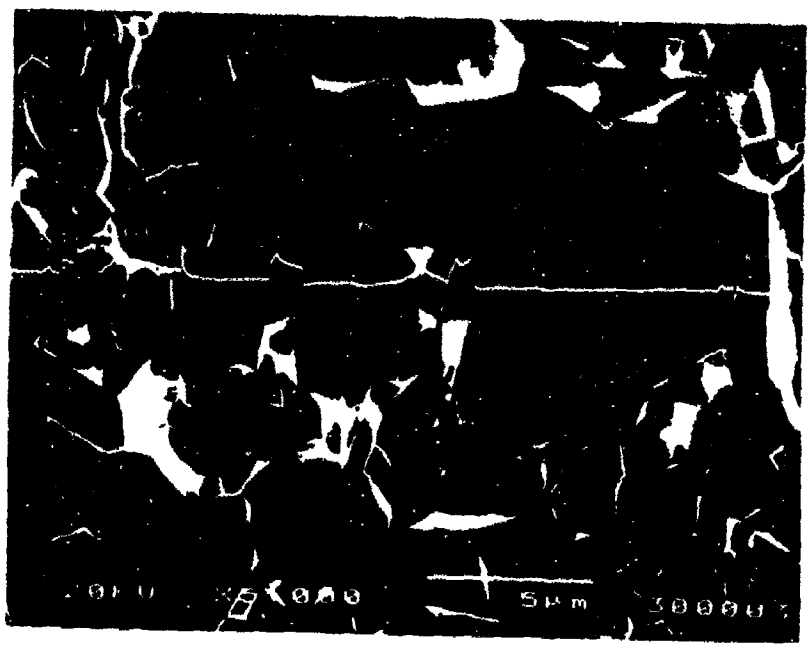

(b) Rapid Crack Growth

Figure 5. SEM and LSP Traces of Alumina

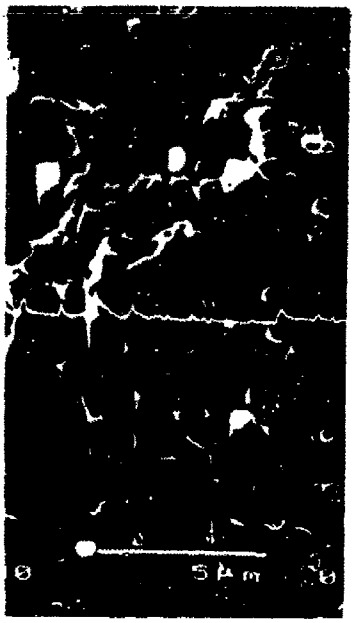

(a) Stable Crack Growth

(b) Rapid Crack Growth

Figure 6. SEM and LSP Traces of SiC $_w$/ Al_2O_3 Composite

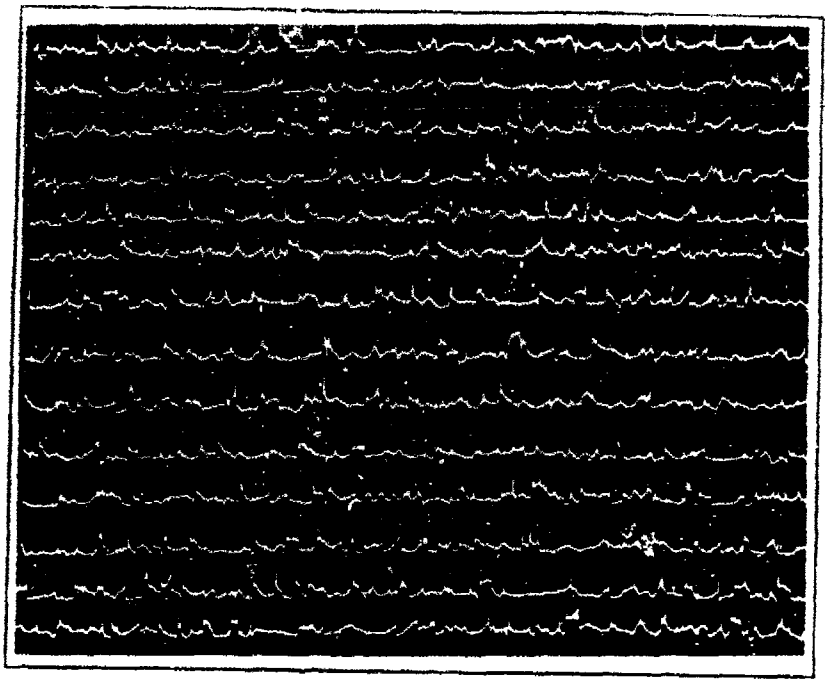

(a) Stable Crack Growth

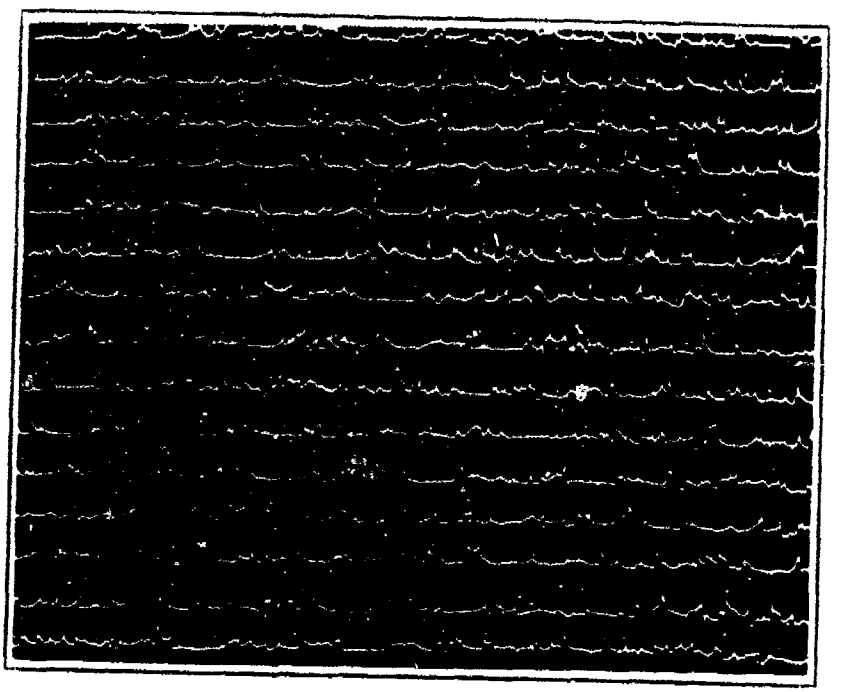

(b) Rapid Crack Growth

Figure 7. Line Scanning Profiles of Stable and Rapid Crack Growth in Alumina

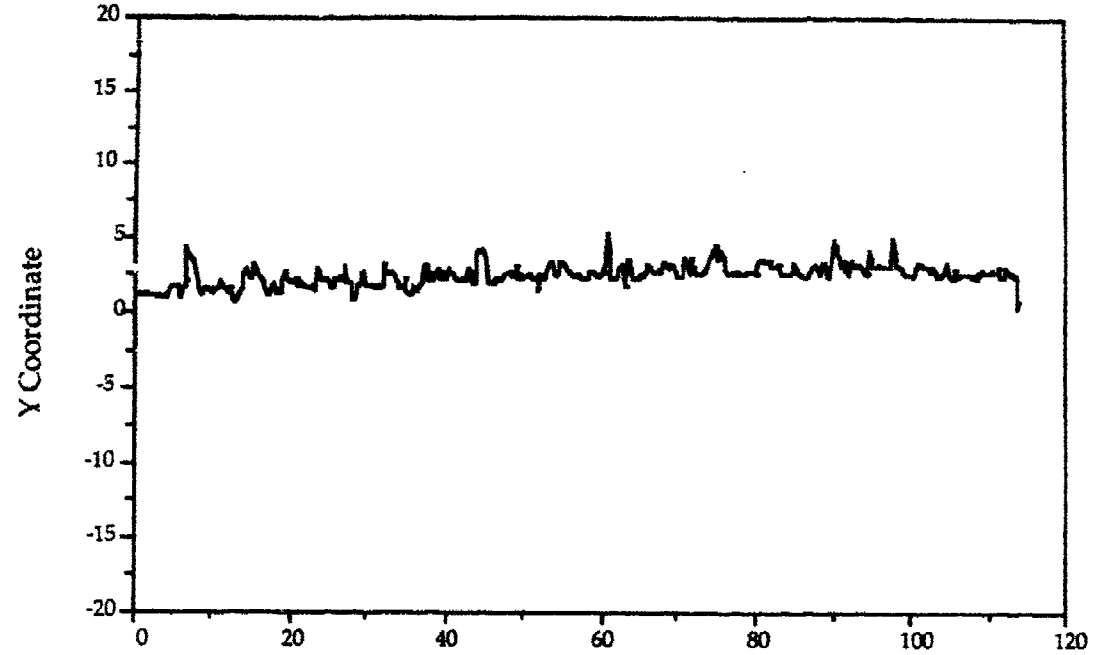

(a) Stable Crack Growth

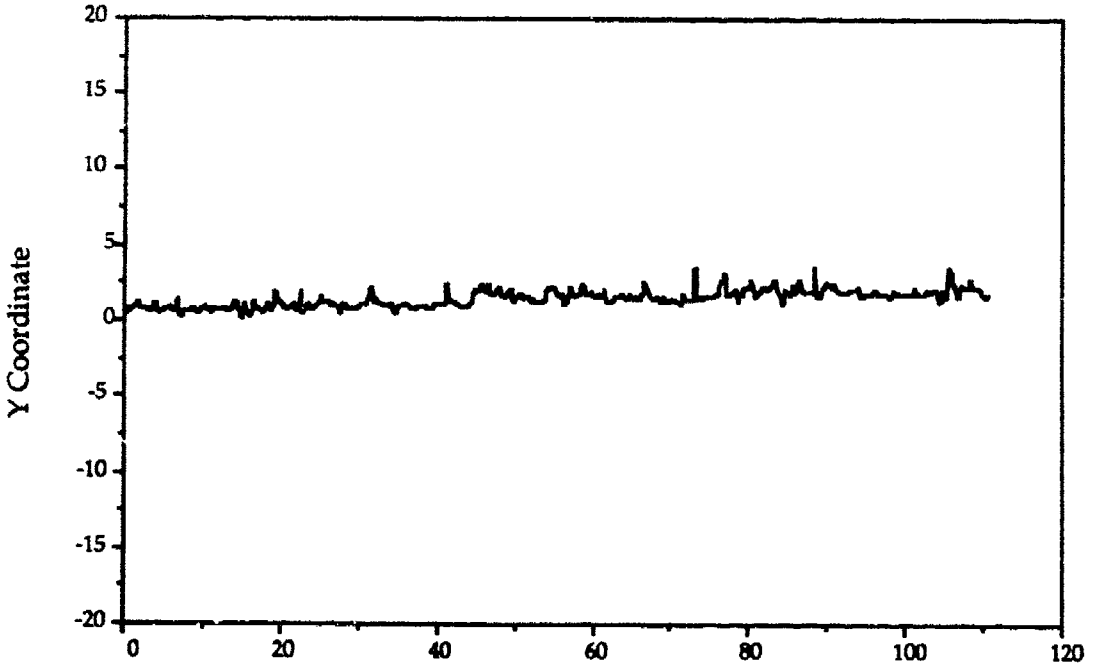

(b) Rapid Crack Growth

Figure 8. Line Scanning Profiles of Stable and Rapid Crack Growth in SiC_w/Al_2O_3 Composite

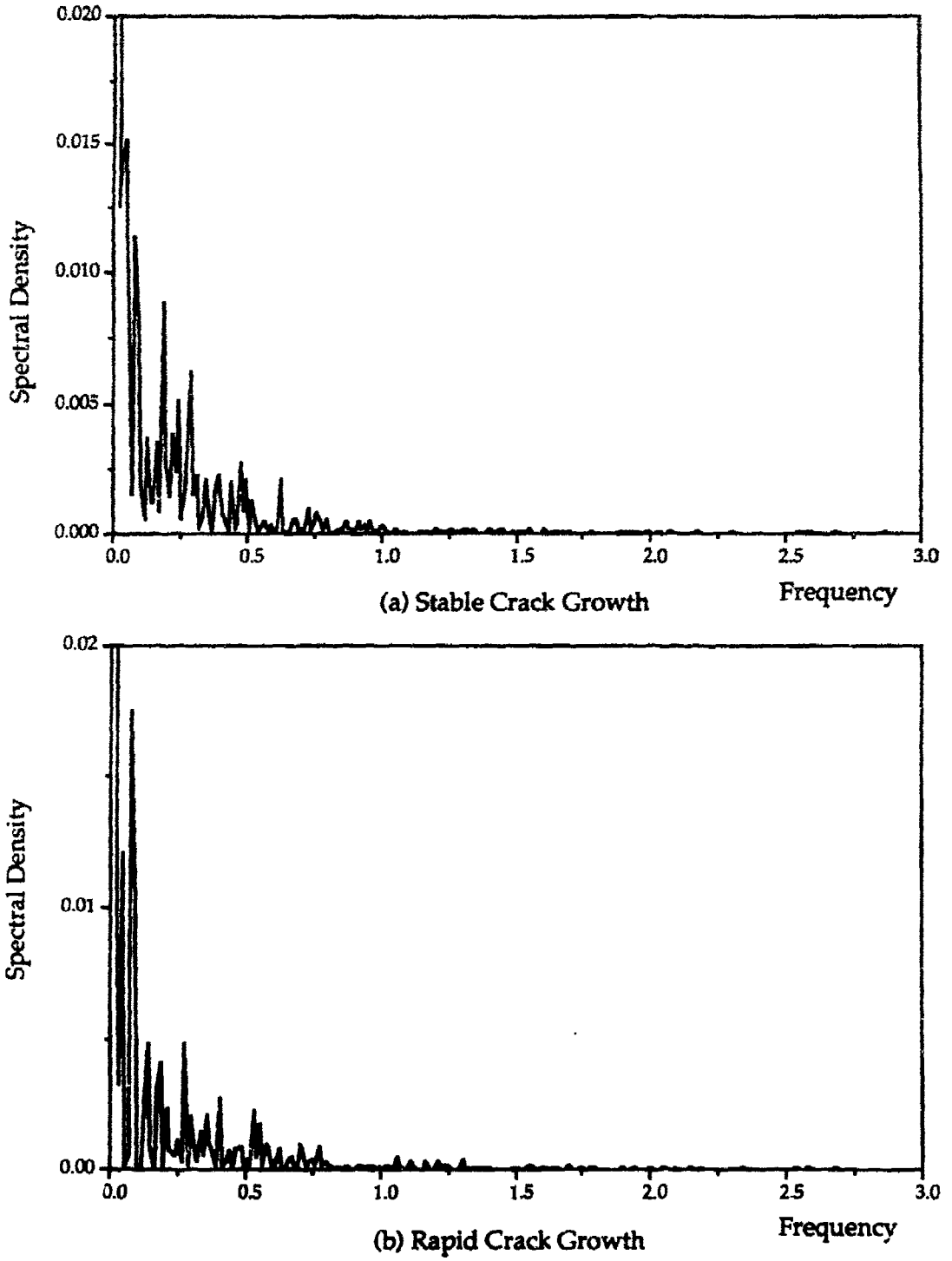

Figure 9. LSP Spectral Density of Stable and Rapid Crack Growth in Alumina

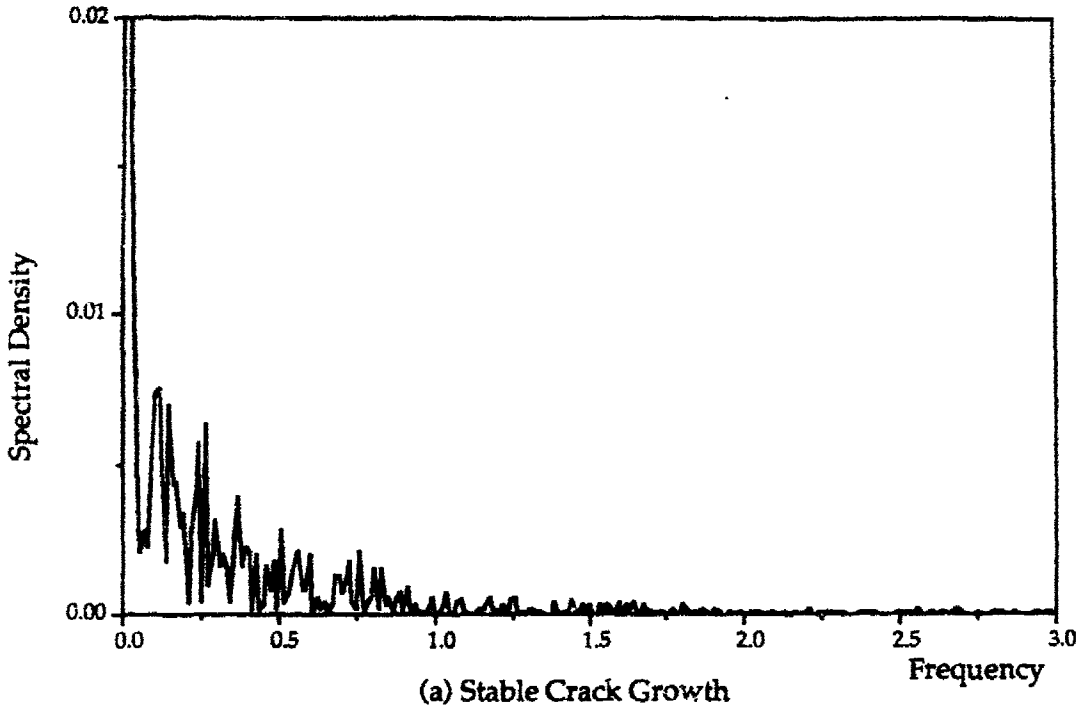

(a) Stable Crack Growth

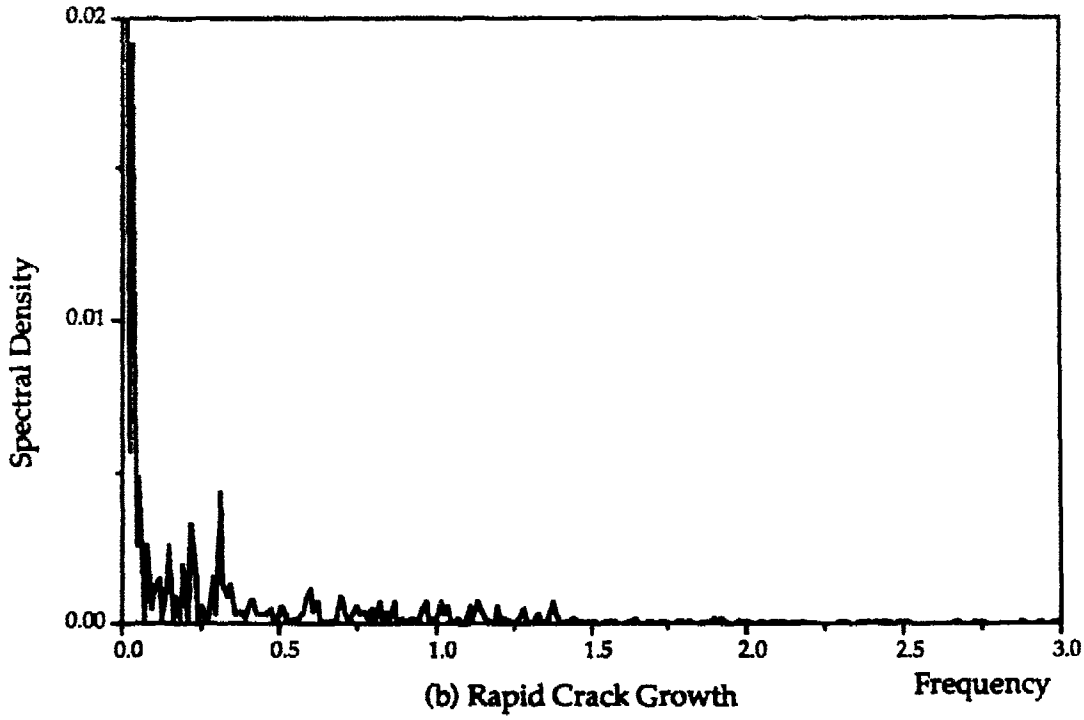

(b) Rapid Crack Growth

Figure 10. LSP Spectral Density of Stable and Rapid Crack Growth in SiC_w/Al_2O_3 Composite

SECURITY CLASSIFICATION OF THIS PAGE (When Data Entered)

REPORT DOCUMENTATION PAGE

READ INSTRUCTIONS BEFORE COMPLETING FORM

1. REPORT NUMBER	2. GOVT ACCESSION NO.
3. RECIPIENT'S CATALOG NUMBER: UWA/DME/TR-90/3	
4. TITLE (and Subtitle): A SEM Procedure for Quantifying Transgranular Fracture in Brittle Material.	5. TYPE OF REPORT & PERIOD COVERED: Technical Report
	6. PERFORMING ORG. REPORT NUMBER: UWA/DME/TR-90/3
7. AUTHOR(s): W.-J. Yang, C.-T. Yu and A.S. Kobayashi	8. CONTRACT OR GRANT NUMBER(s): N00014-87-K-0326
9. PERFORMING ORGANIZATION NAME AND ADDRESS: Dept. of Mech. Engr., FU-10 University of Washington Seattle, WA 98195	10. PROGRAM ELEMENT, PROJECT, TASK AREA & WORK UNIT NUMBERS
11. CONTROLLING OFFICE NAME AND ADDRESS: Office of the Chief of Naval Research Arlington, VA 22217-5000	12. REPORT DATE: 7/90 13. NUMBER OF PAGES: 21
14. MONITORING AGENCY NAME & ADDRESS (if different from Controlling Office)	15. SECURITY CLASS. (of this report): Unclassified 15a. DECLASSIFICATION/DOWNGRADING SCHEDULE

16. DISTRIBUTION STATEMENT (of this Report)

Unlimited

17. DISTRIBUTION STATEMENT (of the abstract entered in Block 20, if different from Report)

18. SUPPLEMENTARY NOTES

19. KEY WORDS (Continue on reverse side if necessary and identify by block number)

Fractography, Alumina, ceramic composite

20. ABSTRACT (Continue on reverse side if necessary and identify by block number)

A SEM procedure for quantifying the percentage area of transgranular fracture was developed for studying the fracture morphologies of stable and rapid crack growths in ceramics and ceramic matrix composites. The procedure utilizes SEM line scanning profiles which are scanned and then interpreted as percentage area of transgranular fracture and surface roughness through a special software. This procedure was used to quantify the percentage area of transgranular fracture and sruface roughness which were correlated with the visual observations and profilometer measurements respectively, of Al_2O_3 and SiC_w/Al_2O_3 fracture specimens

DD FORM 1 JAN 73 1473 EDITION OF 1 NOV 65 IS OBSOLETE
S/N 0102-014-6601

Unclassified
SECURITY CLASSIFICATION OF THIS PAGE (When Data Entered)